Astron. Astrophys. 321, 549–556 (1997)

ASTRONOMY
AND
ASTROPHYSICS

The gas-dynamic model of impulsive stellar flares

M.M. Katsova[1], **A.Ya. Boiko**[2], **and M.A. Livshits**[3]

[1] Sternberg State Astronomical Institute, Moscow State University, 119899 Moscow, Russia (maria@sai.msu.su)
[2] Space Research Institute of Russian Academy of Sciences, Profsoyuznaya 84/32, 117810 Moscow, Russia (aboiko@mx.iki.rssi.ru)
[3] Institute of Terrestrial Magnetism, Ionosphere, and Radio Wave Propagation, Russian Academy of Sciences 142092, Troitsk, Moscow Region, Russia (livshits@izmiran.rssi.ru)

Received 7 May 1996 / Accepted 20 October 1996

Abstract. We investigate the response of a plasma in a magnetically confined loop to intense impulsive energy release during stellar flares. We carry out a numerical simulation of gas-dynamic processes in an approximation to a single-fluid, two-temperature, plasma with a possible distinction between the ion and electron temperatures taken into account. We present here results of the modelling for an initial model of the red dwarf atmosphere including the photosphere, the chromosphere, the transition region and the corona. Tenuous layers of the upper chromosphere, which usually exist in quiescent regions on red dwarfs are also included in this initial model. This is a fertile field for development of our understanding of the process of explosive evaporation.

Heating of the plasma is due to a hard electron beam with an energy of $3 \cdot 10^{11}$ erg cm^{-2} s^{-1}; this value is based on an analysis of the soft X-ray data for stellar flares. The use of a new numerical technique reveals basic features of the gas-dynamic processes for a single, elementary, heating lasting 10 s. In the first 0.1 - 0.2 s, the plasma is heated strongly in the upper chromospheric layers, followed by two disturbances which subsequently propagate downward and upward from the high-pressure region formed. A flow quickly follows, with a temperature jump which moves slowly downwards, and ahead of which travels a radiative shock wave. Also, hot gas moves outwards from the region of the temperature jump. Modelling allows us to determine the physical conditions at the source of the emission in different spectral regions, and, in particular, it provides evidence for the thermal origin of optical emission from stellar flares.

We discuss possibilities for the interpretation of observational data of real stellar flares which consist of a set of elementary events. This modelling has the advantage that the behaviour of the optical, EUV and soft X-ray radiation can be explained simultaneously.

Our gas-dynamic modelling may be applied to impulsive stellar flares with amplitudes $\Delta U < 3^m$, i.e. until thermal conduction fluxes are smaller than the saturated ones and the return current doesn't limit the penetration of accelerated electrons into the chromosphere.

Key words: red dwarf stars – stellar flares – gas-dynamic modelling

Send offprint requests to: M.M. Katsova

1. Introduction

Many of our general conceptions concerning the analogy between flares on the Sun and the UV Cet-type stars (active red dwarf stars) derive from Gershberg & Pikel'ner (1972). When an impulsive flare on the Sun is considered, it is necessary to keep in mind the hard ($E \geq 20$ KeV) X-ray burst. Several spikes can be observed during ≈ 100 s. As a rule, a single short spike is an event, which occurs in a low-lying (< 10000 km) loop. The total duration of a hard X-ray burst is controlled by the development time of the flare process as a whole in the system of coronal loops.

The hard X-ray radiation is due to the bremsstrahlung emission of accelerated electrons. These particles and the heat fluxes which arise in the region of primary energy release affect the chromosphere. The response of the solar chromosphere to the impulsive heating, the so called secondary process in a flare, was computed by Kostyuk & Pikel'ner (1974), where the importance of gas-dynamic motions was demonstrated for the first time. Later, a number of scientific groups have carried out analogous computations for the Sun (Kopp et al. 1989, and, in particular, Fisher et al. 1985). The main results of this modelling were confirmed by many solar observations.

Direct observations of the hard X-ray flare emission on red dwarf stars are in their infancy. However, our knowledge of, and the observational data on, stellar flares, makes it possible to assume that impulsive heating of the upper chromosphere takes place also during short events on red dwarf stars. This heating can be caused by electron beams as well as other factors, and it can lead to a development of secondary processes analogous to

the solar ones. The first numerical simulations of a flare on a red dwarf star was carried out by Livshits et al. (1981) and Katsova et al. (1981). There, it was shown that the optical continuum emission sometimes accompanies the gas-dynamic response of impulsive heating of the chromosphere.

We consider impulsive flares identified with optical continuum bursts. The shortest stellar flares can be the result of a single heating by conduction or by the impact of accelerated electrons onto the chromosphere. This process is referred to as an 'elementary event' which lasts from a few tenths of a second to ten seconds. The real impulsive flare can continue longer, about 100 s and sometimes more, and can be considered as a set of such elementary bursts. In this case the process can envelop several low-lying loops. This is an important point in the interpretation of observational data on stellar flares.

It should be noted that Cheng & Pallavicini (1991) have carried out a series of computations of the response of a stellar chromosphere to heating in the top of a magnetically confined loop. This case of prolonged (a few hundreds of seconds) heating, located in coronal layers, describes well the important physical processes in the corona. These authors calculated the expected X-ray emission and compared it with the X-ray flare light curves obtained with EXOSAT. Trying to interpret the X-ray flare data, Cheng & Pallavicini were restricted to only a qualitative consideration of physical processes in the chromospheric layers close to the footpoints of the loop. Unfortunately, they didn't develop their modelling as applied to chromospheric layers or to an interpretation of optical radiation of stellar flares.

Therefore, we propose a gas-dynamic model for an impulsive flare which is able to interpret data not only in the soft X-ray, but also in the UV range, optical line and continuum emission.

We will discuss here the results of some new numerical modelling of an elementary flare event, when it occurs in the outer atmosphere of the red dwarf star AD Leo. In addition we consider the total effect from the influence of a number of such bursts, and some features of the behaviour of flaring radiation over a wide range of wavelengths.

2. The response of a stellar chromosphere to impulsive heating

Let's consider the processes in the region adjacent to the footpoint of a loop. The particles and heat fluxes propagate along the magnetic lines of force, allowing a one-dimensional approach. The initial structure of the stellar atmosphere contains a corona, a transition region, a chromosphere and a photosphere. We consider the loop to be like a vertical tube with a constant cross-section with height. We suppose that the flux of the accelerated electrons is injected into the loop from above. The gas-dynamic processes which develop in this structure are analyzed.

The main problem confronting the modelling of impulsive processes is the computation of the characteristics of a region of very high temperature gradient. Additional assumptions were adopted such as the continuity of the pressure $p(z)$ in the region of the temperature jump (thermal conduction front), a different dependence of the degree of ionization on the temperature in front of and behind this jump. Taking into account our previous experience of numerical simulation, we have changed the statement of the problem in the following way: namely we abandon any attempt to describe the region of the temperature jump, and use a unified dependence of $x(T)$ both for the low and high temperature layers.

Previous experience of gas-dynamic modelling of solar and stellar flares, leads us to use a single-fluid approach to a description of gas-dynamic processes in a collision dominated chromospheric and coronal plasma. Similar time dependent equations are used by Cheng in all his computations (Cheng et al. 1983). In principle, we could also restrict the model to a single-temperature approximation (Katsova et al. 1981); a two-temperature approach gives qualitatively the same solution, but allows us to determine more exact quantitative values of physical parameters which are characteristic of the flare process, such as the density, the temperature, and the thermal conduction flux. For a comparison between two- and single-temperature computations for a solar flare see in Boiko & Livshits (1995).

The set of equations for a two-temperature, single-fluid plasma is as follows:

$$\frac{dn}{dt} + n\frac{\partial v}{\partial z} = 0, \tag{1}$$

$$mn\frac{dv}{dt} = -\frac{\partial}{\partial z}(p_i + p_e - q) - mgn, \tag{2}$$

$$n\frac{d}{dt}(x\varepsilon_e) + p_e\frac{\partial v}{\partial z} + \frac{\partial W}{\partial z} = P_e + P_0 - L - Q, \tag{3}$$

$$n\frac{d\varepsilon_i}{dt} + (p_i - q)\frac{\partial v}{\partial z} = Q. \tag{4}$$

Here the ratio of the specific heats for hydrogen plasma is $\gamma = 5/3$; the internal energy of the electron component is $\varepsilon_e = \frac{k}{(\gamma-1)}T_e + \chi = \frac{3}{2}kT_e + \chi$; the internal energy of heavy particles is $\varepsilon_i = \frac{k}{(\gamma-1)}T_i = \frac{3}{2}kT_i$ (here it is assumed that the temperature of neutral atoms is the same as that of protons), where χ is the ionization potential of hydrogen, n is the density of equivalent hydrogen atoms (i.e. $n = N(H1) + n_p$), $n(H1)$, n_p, $n_e = n_p$ are densities of neutral hydrogen, protons and electrons respectively; $x = n_e/n$ is degree of ionization; $q = \frac{4}{3}\eta\frac{\partial v}{\partial z}$ is the viscosity; η is viscosity coefficient; $W = -\kappa\frac{\partial T_e}{\partial z}$ is thermal conduction flux, where κ is the thermal conduction coefficient; P_e is heating function; L is radiative cooling function; P_0 is heating balancing the radiative losses at the initial time, and Q is the energy exchange function between the electron and ion components.

The following boundary conditions apply: static upper and lower boundaries, an absence of thermal conduction fluxes;

$$v(t, \xi_{min}) = v(t, \xi_{max}) = 0,$$

and

$$\frac{\partial T_e}{\partial z}(t, \xi_{min}) = \frac{\partial T_e}{\partial z}(t, \xi_{max}) = 0.$$

Here the number of the hydrogen nuclei in the column, determined above, $\xi = -\int_z^\infty n\,dz$, is the Lagrangian coordinate.

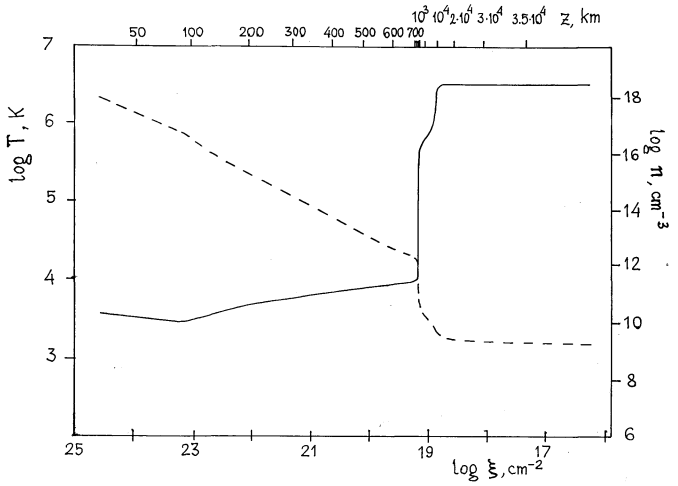

Fig. 1. The distribution of temperature (solid line) and the density (dashed line) shown as a function of the column number for the initial model (see references in the text). The horizontal axis at the top of the figure represents heights above the level where $\tau_{5000} = 1$ for this initial model.

As the initial model we use the Hawley-Fisher's QT3 model (1992), where the photosphere, the chromosphere and the transition region are included. The densities are small enough in the upper layers of the QT3 model (column mass above the transition region m_0 in g cm^{-2} is $\log m_0 \approx -4.4$). We add the coronal layers to this model up to heights of 30 000 km in accordance with Katsova et al. (1987). The distribution of the parameters of the initial model are shown in Fig. 1.

We suppose that the chromosphere is heated by an electron beam of energy $3 \cdot 10^{11}$ erg cm^{-2} s^{-1} and the time profile of the heating flux has a rectangular form. The value of the heating flux F_0 is set to agree with the soft X-ray flux for stellar flares. We choose the spectrum of the electrons hard enough as compared with typical one, detected from the hard X-ray bursts on the Sun. Namely, we assume $vN(E) \propto E^{-3}$, where v is the velocity of the electrons, E is their energy, and $N(E)$ is the differential spectrum. For hard solar bursts, $N(E)$ is proportional to E^{-2} – E^{-6}. An injection of this electron beam into the chromosphere leads to a heating distributed over the Lagrangian coordinate. The level of heating is evaluated according to Syrovatskii & Shmeleva (1972). The results of our gas-dynamic modelling remain valid for any mechanisms of powerful impulsive heating not only for electron beams, but also others, such as an absorption of impulsive X-ray radiation, etc, which affect the heating distributed over the Lagrangian coordinate.

It is necessary to consider the gas-dynamic processes in a stellar atmosphere taking into account the radiation of the plasma. At lower temperatures, radiative losses and the degree of ionization are computed using the results from a consideration of the kinetics of the hydrogen atom in layers with a given optical depth at the centre of the L_α - line (Bruevich & Livshits (1993)). The same function $x(T)$ as the one calculated for the layer with $\tau(L_\alpha) = 10^3$ is used now in the gas-dynamic modelling for all layers with different optical depths. Although it leads to a small overestimate of the temperature of the layers below the transition region, the assumption that the degree of ionisation is independent of optical depth over a range in column number allows us to avoid consideration of a complete set of radiative gas-dynamic equations, and to restrict our approach to a typical set of equations, where the radiation has only dissipative terms in the energy equation.

The radiative cooling function for the temperatures $T >$ 15000 K is taken from Raymond & Smith (1977), (see the details in Boiko & Livshits, 1995). The heating of the initial atmosphere is calculated as

$$P_0(n, T_e) = xn^2 L(T_e(\xi, 0))$$

The energy exchange between the electron and the ion components of the plasma is

$$Q \approx 1.48 \times 10^{-17} {n_e}^2 (T_e - T_i) {T_e}^{-3/2}$$

The final expression for the heating flux and radiative loss function can be found in Boiko & Livshits (1995). The degree of the ionization $x(T)$ is taken from Bruevich & Livshits (1993) for the layer with $\tau(L_\alpha) = 10^3$. The values of $x(T)$ are distinguished from given ones in Boiko & Livshits (1995) by a factor of 0.9 for $T = 8000 - 12000$ K.

Numerical solution of the set of equations (1)-(4) is troublesome. This problem cannot be solved solely in Lagrangian coordinates. Therefore, for a more exact computation of the motions of the shock wave and thermal conduction front, we compute the motions of the knots of a numerical grid. The numerical method uses the Langangian approach with a re-interpolation of all the functions at each time-step to form a new grid with a new set of physical parameters for the knots (Boiko & Livshits, 1995). Of course, this gas-dynamic problem is a multi-parameteric one; its final solution is sensitive to the degree of heating, the kind of heating agent (accelerated electrons or thermal flux), the hardness of the electron beam, and to the choice of the initial model. The dependence of the solution on the parameters adopted have been investigated for the solar case (see a review by Fisher (1986); Kosovichev et al. 1980). In particular, the density in the source of the optical continuum emission is proportional to the heating flux. Effects in the chromosphere are more remarkable in the case of heating by a hard electron beam, while those in the corona are more pronounced for the case of heating by the softer electron beam. Solutions for small heating fluxes and/or soft electron beams lead to low values of the density and temperature in the source of the optical radiation; therefore they are less useful for stellar flare modelling. For a variant that is close to the computation by Cheng & Pallavicini (1991) (where the initial heating expands to coronal layers above the transition region) we obtain similar results. This paper contains results of the alternative model with a powerful initial heating expanding up to the upper chromosphere. The latter is realized by a choice of the initial model with $\log m_0 \approx -4.4$.

For stellar flare modelling, it would be of interest to carry out the computation with higher values of heating fluxes; however, the thermal flux saturates, and return electric currents arise that

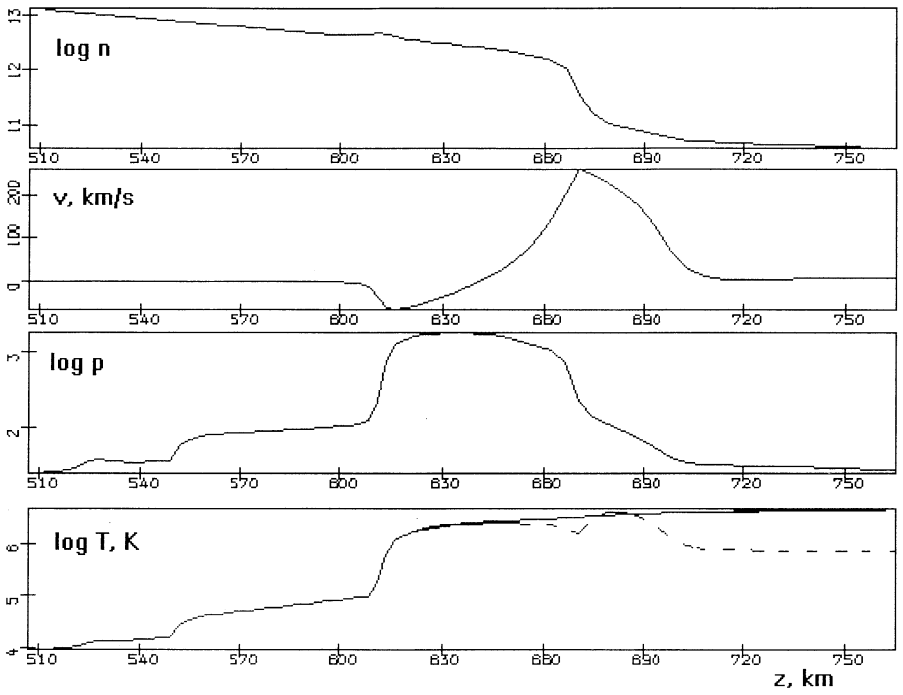

Fig. 2. Distributions of the density, velocity, total pressure and temperatures (electrons - solid line, ions - dashed line) versus height for the time t = 0.1 s after the beginning of the heating. Negative values of velocities correspond to motions toward the photosphere.

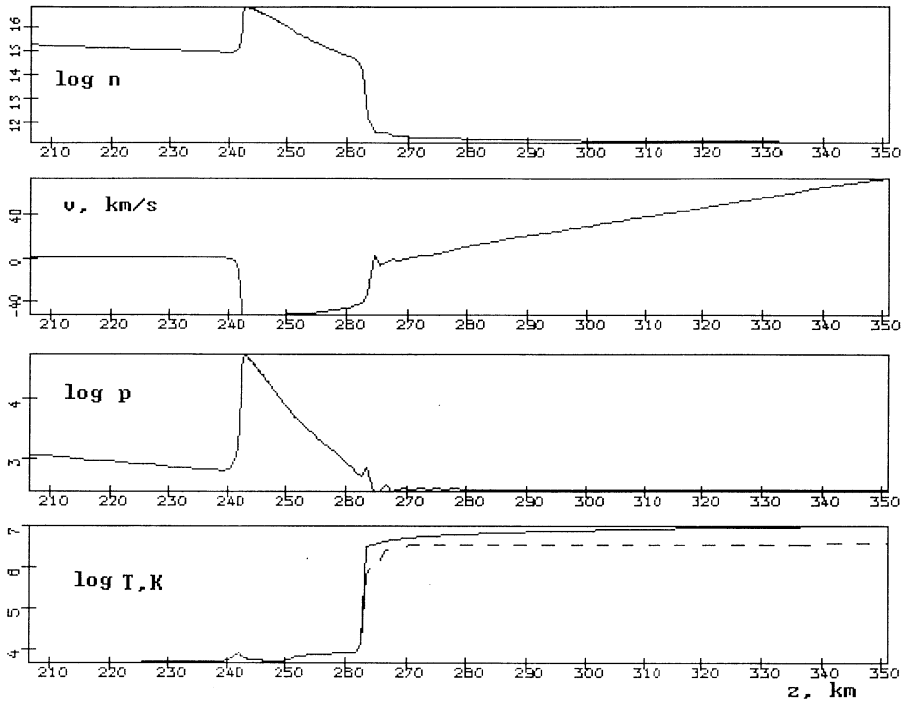

Fig. 3. The same parameters as in Fig. 2, but for the time t = 4 s after the beginning of the heating at the height 242 km above the photosphere.

restrict the penetration of accelerated electrons into the chromosphere. Boiko & Livshits (in prep) tried to take into account these new effects for solar flares. We enlarge here on the model with a heating flux $F_0 = 3 \cdot 10^{11}$ erg cm^{-2} s^{-1} where these effects can be neglected.

2.1. Explosive evaporation of an elementary burst

The conditions for explosive evaporation (Fisher et al. 1985), when the heating time scale in the evaporating region is less than the time scale of hydrodynamic expansion, are assumed to be satisfied in our case of powerful impulsive heating. This process consists of two parts: at the flare onset, in the first 0.1 - 0.2 s, a plasma is heated strongly in the upper chromospheric layers. In this phase there is no motion, the density is constant and the pressure increases sharply. This situation is presented in Fig. 2 for the time t = 0.1 s after the commencement of heating. The region of high pressure is seen at heights 610 - 670 km above the stellar photosphere. Then, 0.3 s after the

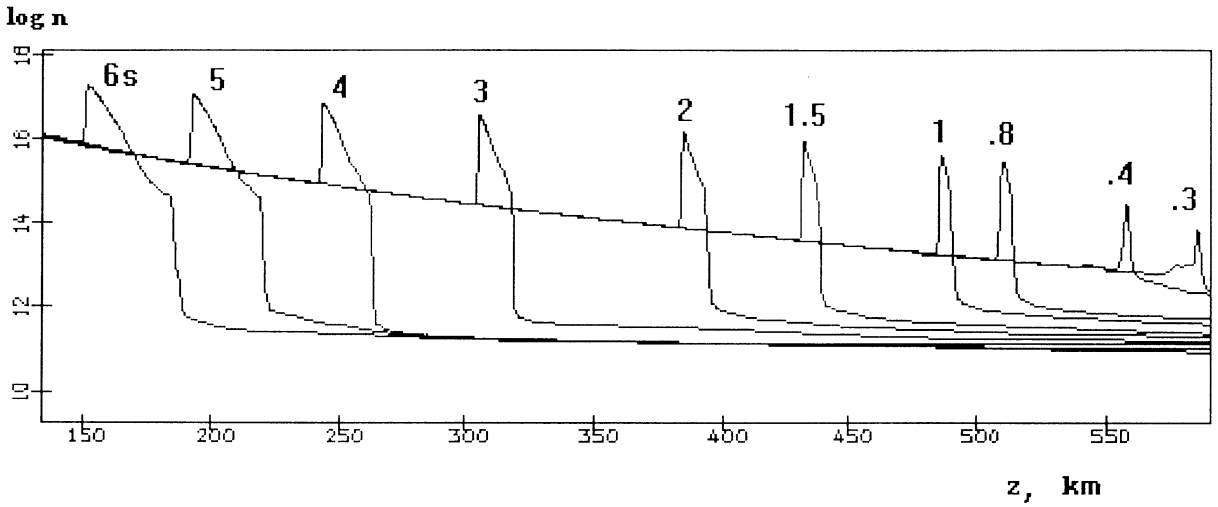

Fig. 4. The density profiles versus the height. The time in seconds is denoted in the upper part of the figure. The straight line refers to the initial model.

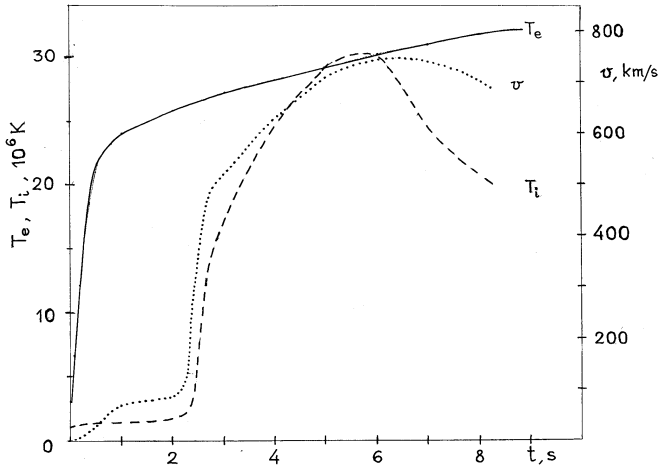

Fig. 5. The time dependence of the electron temperature (solid line), the ion temperature (dashed line) and velocity of the upwards evaporated plasma (dotted line) in the upper part of the flow (at the height 5000 km). The shock front reaches this level 6 s after the flare onset.

flare onset, two disturbances subsequently propagate upward and downward from this high-pressure region.

An important feature of this part of the process is the formation of a region with $T \sim 10^5$ K at heights 550 - 610 km and $\Delta\xi = 3 \cdot 10^{19}$ cm^{-2}. The downward shock wave arises at $t = 0.2$ s, just below the temperature jump, and travels through all the quasi-equilibrium regions with $T \leq 10^5$ K.

The second part of the process of explosive evaporation is characterized by the slow downward motion of a temperature jump, ahead of which a shock wave travels. Hot gas moves outwards from the temperature jump. Our solution is shown in Fig. 3 for $t = 4$ s. The gas behind the downward radiative shock front is compressed by a factor of about 100, and the geometrically thin low-temperature condensation arises between the shock wave and thermal conduction front. It is identified as the source of the low-temperature radiation of flares. The temperature is distributed non-uniformly inside the downward moving condensation: at 4 s it reaches about 8000 K behind the shock front (at the height 242 km) and increases up to 10000 - 12000 K at the top of the condensation, at 262 km, where the thermal flux is able to penetrate. The temperature in the middle of the condensation can be as low as 5000 K. Therefore the flare optical continuum and the Balmer line emission can arise only in the upper and lower layers of the condensation.

Such a distribution of the temperature with a rise at the top and at the bottom of the optical emission source is typical, particularly for a source forming during the gas-dynamic process, when heating is switched on. If this powerful heating is stopped, as in the gradual phase of the flare, it becomes necessary to take into account absorption of the outer X-ray emission. If this effect is considered (Hawley & Fisher, 1992), the temperature stays high enough ($T \approx 8000$ K) over all the condensation, and the gas begins to emit effectively in the optical, not only in outer parts, but also in the inner regions.

The propagation of the low-temperature condensation downward through the AD Leo atmosphere is presented in Fig. 4. The velocities of the cool gas vary gradually from 160 km s^{-1} at 0.4 s to 18 km s^{-1} at 8 s. Note that in all former computations maximal densities didn't exceed 10^{16} cm^{-3}. Their increase here at $t > 3$ s is due to choosing of a variant of the solution, in which weak disturbances from the downward moving temperature jump maintain the shock wave. In many real flares the shock wave can attenuate at $t > 3$ s faster that it is shown in Fig. 4.

The physical parameters in the upward flux at a height of 5000 km are presented in Fig. 5. The electron temperature T_e rises to $20 \cdot 10^6$ K during the first 0.5 s. The ion temperature remains low until the shock wave arrives at this height. The shock front velocities change from 2000 km s^{-1} for $t = 0.28$ s to about of 1000 km s^{-1} for $t = 8.5$ s. When the shock front reaches the given height of 5000 km, the ions heat up strongly

(up to $T_i > T_e$), and the ion temperature becomes close to the electron temperature (see Fig. 5). At this height the velocities of the gas exceed 700 km s^{-1} upwards. The evaporated hot gas moving upwards gradually fills the coronal part of the loop. The flux of the particles is about $5 \cdot 10^{18}$ particles cm^{-2} s^{-1}. This flux of evaporated material increases quickly ($t \leq 1$s) and then remains constant; thus, the mass loss from unit area (1 cm^2) during the entire elementary burst is about $5 \cdot 10^{19}$ particles. The ion temperature of the flare plasma remains lower than the electron temperature in the average over the loop. If we consider the gas-dynamic process, even in a diverging coronal part of the loop, then values of velocities, temperature and mass loss from a unit area (1 cm^2) will be little changed (Getman & Livshits, 1996).

2.2. The properties of the flare radiation accompanying the elementary gas-dynamic process

The low-temperature condensation arises in a few tenths of a second after the flare onset. Physical conditions therein are such that the condensation can emit both in the optical continuum and in the Balmer lines (Livshits et al. 1981; Katsova et al. 1981).

The densities inside the low-temperature condensation are high enough (more than 10^{16} cm^{-3}, Figs. 3 and 4), and physical conditions therein are close to LTE. This is favourable to the production of optical continuum. Gas-dynamic modelling is carried out for a heating flux of 3 times less than in our previous computation. Nontheless, the optical depth of the condensation, in optical continuum at $\lambda \approx 4500$ Å, remains close to 1. Optical continuum emission arises 2 s after the flare onset and lasts a few seconds. The absorption of the soft X-rays in the condensation should lead to an increase in the duration of the optical continuum emission. Thus, this condensation is a source of radiation over a wide spectral range from the optical to the UV (2000 Å).

Theoretical modelling of a flare with optical and UV (2000−3000 Å) observational data confirms our ideas about the thermal origin of flaring optical continuum. This allows us to estimate with confidence the flare area. For the flare of $\Delta U = 2^m$ on the AD Leo, we compute its area as $\approx 5 \cdot 10^{18}$ cm^2, if we adopt the physical conditions of the emission source as in Fig. 3.

The first lines of the Balmer series should be broadened due to the Stark effect. The calculations show that typical FWHM of these lines are close to 4 Å, 2 s after the flare onset. Sometimes the upper part of the condensation can emit an intensive narrow ($1 - 2$ Å) H_α-line. The red shift of the Balmer lines should be small in accordance with small velocities of the downward gas motions. The necessary consequence of the model is that the flare optical continuum emission appears at the time when the slope of the Balmer decrement becomes less steep, independently of the parameters of the emission source. The first consideration of this problem based on the gas-dynamic modelling (Katsova et al. 1991) is given by Katsova (1990), and these results are confirmed by new the solution.

In response to the heating of the chromosphere an emitting region should be formed with a temperature of about 10^5 K. The source of the UV lines like C IV, He II, etc. appears at the flare onset and should exist for several tenths of a second (Fisher, 1987; observations of stellar flare with the ASTRON satellite by Burnasheva et al. 1989 and their interpretation by Katsova & Livshits, 1989), see Fig. 2. According to our computation, the column density of this source is $\Delta\xi \approx 3 \cdot 10^{19}$ cm^{-2} for $t = 0.1 - 0.3$ s. The optical depth at the centre of the resonant C IV line $2p\ ^2P^0_{3/2} - 2s\ S_{1/2}$ is $1.5 \cdot 10^{-17}\Delta\xi \approx 450$. For these conditions, the source function is close to the Planck function, and the flux at the Earth in both lines of the C IV doublet can be estimated as

$$F(CIV) = \frac{2\pi B_\lambda(T) 3\Delta\lambda_D S}{2\pi d^2} \quad (5)$$

where d is the distance to the star (for the AD Leo d = 4.9 pc), the width of the C IV line is $3\Delta\lambda_D, and\ B_\lambda(T)$ is the Planck function. If we suppose that the area of the UV-line emission is the same as in the optical continuum emission the C IV doublet line flux is $\approx 10^{-9}$ erg cm^{-2} s^{-1} for AD Leo. Such a flux should accompany the beginning of this process in each elementary burst. A fast burst like this should be observed in the He II 304 Å and possible in some other lines.

The UV emission doesn't end after the formation of the shock wave. The plasma with a temperature of $(1-4) \cdot 10^6$ K in the lower part of the evaporated flow is the source of the EUV lines in the first few seconds after the beginning of the process. These lines have to be broadened by the Doppler effect, but they shouldn't have significant blueshift. The blueshifted component of the high-temperature lines observable during flares are those emitted by ions such as Fe XXIV and Ca XIX. The intensities of the EUV lines depend on the flare area, which is close to the area of the optical continuum source. The rise of the intensity of these lines occurs 1-2 s ahead of the appearance of the optical continuum and about 3 - 10 s ahead of the soft X-ray radiation during powerful events with duration no longer than a few minutes (i.e. such events can be considered as a response to a single act of primary energy release). The soft X-ray emission is due to hot gas evaporated upwards. For a given particle flux of $5 \cdot 10^{19}$ particles cm^{-2} s^{-1} and the area of one footpoint of the loop, mentioned above, the emission measure of hot gas per one elementary burst is estimated as 10^{50} cm^{-3}. It is clear that in order to provide the observed value of the emission measure we need a set of elementary bursts. These results concerning the evaporation of hot flaring plasma agree well with the computations by Cheng & Pallavicini (1991) for red dwarf stars.

2.3. The result of a set of elementary events

The injection of an electron beam into a given point of the stellar chromosphere lasts, probably, not more than several seconds. This can be repeated, both in the second footpoint of the same low-lying loop, and in some adjacent loops. The hard X-ray data on solar flares, observed with high temporal and spatial resolution, show that all impulsive flares consist of a number of elementary events, and that these spikes are distributed randomly during the impulsive flare.

The above discussed gas-dynamic processes are subsequently developed in several low-lying loops of active regions on the star. The total radiation of an impulsive flare can be the sum of the emission accompanying several single, elementary acts of primary energy release. It includes few additional components. First, each elementary gas-dynamic process relaxes during tens of seconds due to the propagation of the disturbance into the photosphere. In single bursts, the intensities of optical continuum and broad lines decrease slowly after the end of heating. Usually, the total duration of powerful impulsive flare is about of 100 s, which includes several elementary events and their decline. Second, the observable soft X-ray emission should arise in tens of seconds after the beginning of the flare as the plasma is evaporated from the chromospheric footpoint to the corona during 1-3 elementary bursts.

The soft X-ray emission can last longer. This is determined by the radiative loss rate and the efficiency of the process of heat conduction along the loop from coronal levels downwards. The characteristic times of both processes are close to each other, and are equal to

$$t_{rad} = 3kT/n_e L(T) \ ,$$

where n_e and T are the electron density and the temperature of flaring plasma, and $n^2 L(T)$ is radiative loss per cm^3 (see also Pallavicini et al., 1990).

3. Discussion

Modern computational techniques allow us to investigate with confidence the response of the atmosphere to the impulsive heating. Now we have the numerical method, that takes into account all the main physical processes such as thermal conduction, radiative cooling, stellar gravity, etc, and which gives an adequate description of the flare process for a given mechanism of heating and a chosen initial model of the stellar atmosphere. This paper presents one typical variant of the computation for a flare on AD Leo where conditions are favourable for the appearance of flare optical radiation.

Two features of this gas-dynamic modelling should be pointed out.

First, these results remain valid when impulsive heating is located in layers which include the upper chromosphere (under the transition region). This is significant if the flaring process is considered in a real outer atmosphere of a late-type star containing a chromosphere and a corona. It is fulfilled in our numerical modelling because we consider an outer atmosphere with a transition region at $\xi \approx 2 \cdot 10^{19}$ cm^{-2} (the column mass $\log m_0 \approx -4.4$), and a maximum of the energy release of accelerated electrons with $E > 10$ KeV, below or near the transition region.

In fact, the initial atmospheric model adopted here relates to a quiescent red dwarf (dM) star (without emission in its optical spectra) as seen in a set of chromospheric models by Houdebine et al. 1995. Thus, flare optical continuum is generated effectively when accelerated electrons with $E > 10\ KeV$ impact on the chromosphere with a moderate activity level ($\log m_0 = -4.4$, see Houdebine et al. 1995) or electron beams of higher energies impact onto the active dense chromosphere ($\log m_0 = -3$). In the case when heating doesn't expand the upper chromopshere, we obtain the solution that is close to one given by Cheng & Pallavicini (1991). Then, when heating occurs in coronal layers, the L_x/L_{opt} ratio should exceed the value corresponding to our solution, given in Fig. 3.

Second, we consider here a level of heating by accelerated electrons, for which thermal fluxes during the developing gas-dynamic process don't exceed the corresponding saturated heat flux. This condition limits the energy flux of these particles to 10^{11} erg cm^{-2} s^{-1} for the hard spectrum we have chosen ($vN(E) \propto E^{-3}$). In addition, we suggest that the energy of the flux of accelerated particles isn't limited by the return currents that can arise when intensive electron beams are injected into the chromosphere. These circumstances allow us to apply the results of these numerical simulations to the interpretation of simultaneous multi-wavelength observations of stellar flares of any power other than the most powerful ones (with $\Delta U > 5^m$).

The gas-dynamic model presented here allows us to interpret observations of flares on red dwarf stars. One of the most important points is the evidence for the thermal origin of flare optical continuum radiation. The calculations show that the source of the optical continuum is formed within several tenths of a second after the flare onset. If the heating is turning-off when the optical radiation appears, this source continues to exist until the shock wave dissipates due to the propagation through a medium with increasing density. The time for the dissipation is about of 0.5 s. Therefore, the duration of the fastest bursts of optical continuum should be less than 0.5 s.

On the other hand, really large impulsive flares can be presented as a series of elementary bursts. An injection of accelerated electrons into the chromosphere can occur as a sequence of fast pulses, partly overlapping in time. The gas-dynamic response then takes place at the footpoints of various low-lying loops. In principle, this numerical modelling gives the possibility to predict the behaviour of light curves in different spectral ranges.

Acknowledgements. We thank Dr.C.J.Butler and the referee, Dr.D.Moss, for remarks which help us to improve the final version of this paper. The work of M.A.Livshits was supported by Federal Program on Astronomy and Russian Foundation of Fundamental Research (grant 96-02-18382).

References

Boiko, A.Ya., Livshits, M.A., 1995, Astronomy Reports, 39, 381
Boiko, A.Ya., Livshits, M.A., in preparation
Bruevich, E.A., Livshits, M.A., 1993, Astronomy Reports, 37, 532
Burnasheva, B.I., Gershberg, R.E., Zvereva, A.M., et al. 1989, SvA, 33, 165
Cheng, C.-C., Oran, E.S., Doschek, G.A., Boris, J.P., Mariska, J.T., 1983, ApJ, 265, 1090
Cheng, C.-C., Pallavicini, R., 1991, ApJ, 381, 234

Fisher, G.H., 1986, in: Radiation Hydrodynamics in Stars and Compact Objects, eds. Mihalas D., Winkler K.-H. Lect.Notes in Physics, Berlin: Springer Verlag, 255, p. 53
Fisher, G.H., 1987, ApJ, 317, 502
Fisher, G.H., Canfield, R.C., McClymont, A.N., 1985, ApJ, 289, 425
Getman, K.V., Livshits, M.A., 1996, Solnechnye Dannye, in press
Gershberg, R.E., Pikel'ner, S.B., 1972, Comments Astrophys. Space Phys, 4, 113
Hawley, S.L., Fisher, G.H., 1992, ApJS, 78, 565
Houdebine E.R., Doyle J.G., Koscielecki M., 1995, A &A, 294, 773
Katsova, M.M., 1990, SvA, 34, 614
Katsova, M.M., Badalyan, O.G., Livshits, M.A., 1987, SvA, 31, 652
Katsova, M.M., Kosovichev, A.G., Livshits, M.A., 1981, Afz, 17, 285
Katsova, M.M., Livshits, M.A., 1989, SvA, 33, 155
Katsova, M.M., Livshits, M.A., Butler, C.J., Doyle, J.G., 1991, MNRAS, 250, 402
Kopp, R.A., Fisher, G.H., MacNice, P., et al., 1989, in: Energetic Phenomena on the Sun, eds. M.R.Kundu, B.Woodgate, E.J.Schmahl, Dordrecht, Kluwer, p. 601
Kosovichev, A.G., Livshits, M.A., Popov, Yu.P., 1980, Preprint of the M.V.Keldysh Institute of Applied Mathematics, No 68, Moscow, 39 pp, (in russian)
Kostyuk, N.D., Pikel'ner, S.B., 1975, SvA, 18, 590
Livshits, M.A., Badalyan, O.G., Kosovichev, A.G., Katsova, M.M., 1981, Solar Phys., 73, 269
Pallavicini, R., Tagliaferri, G., Stella, L., 1990, A&A, 228, 403
Raymond J.C., Smith B.W.,1977, ApJS, 35, 419
Syrovatskii S.I., Shmeleva O.P., 1972, AZh, 49, 334

This article was processed by the author using Springer-Verlag LaTeX A&A style file *L-AA* version 3.